

Cite this article as:

Marcos, J.V., Muñoz-Barrutia, A., Ortiz-de-Solórzano, C. and Cristóbal, G., 2015. Quantitative assessment of emphysema severity in histological lung analysis. *Annals of Biomedical Engineering*, 43(10), pp.2515-2529.

DOI: <https://doi.org/10.1007/s10439-015-1251-5>

Quantitative assessment of emphysema severity in histological lung analysis

J. Víctor Marcos · Arrate Muñoz-Barrutia ·
Carlos Ortiz-de-Solórzano · Gabriel Cristóbal

Received: date / Accepted: date

Abstract Emphysema is a characteristic component of chronic obstructive pulmonary disease (COPD), which has been pointed out as one of the main causes of mortality for the next years. Animal models of emphysema are employed to study the evolution of this disease as well as the effect of treatments. In this context, measures such as the mean linear intercept (L_m) and the equivalent diameter (d) have been proposed to quantify the airspace enlargement associated with emphysematous lesions in histological sections. The parameter D_2 , which relates the second and the third moments of the variable d , has recently shown to be a robust descriptor of airspace enlargement. However, the value of D_2 does not provide a direct evaluation of emphysema severity. In our research, we suggest a Bayesian approach to map D_2 onto a novel emphysema severity index (SI) reflecting the probability for a lung patch to be emphysematous. Additionally, an image segmentation procedure was developed to compute the severity map of a lung section using the SI function. Severity maps corresponding to 54 lung sections from control mice, mice induced with mild emphysema and mice induced with severe emphysema were computed, revealing differences between the distribution of SI in the three groups. The proposed methodology could assist in the quantification of emphysema in animal models.

Keywords Chronic obstructive pulmonary disease (COPD) · Animal models · Parzen window estimation · Lung segmentation · Severity map

J.V. Marcos and G. Cristóbal
Instituto de Óptica, Spanish National Research Council (CSIC)
Serrano 121, Madrid 28006, Spain
E-mail: jvmarcos@gmail.com, gabriel@optica.csic.es

A. Muñoz-Barrutia and C. Ortiz-de-Solórzano
Cancer Imaging Laboratory, Center for Applied Medical Research, University of Navarra
Pío XII 55, Pamplona 31008, Spain
E-mail: arrmunoz@unav.es, codesolorzano@unav.es

1 Introduction

The Global Initiative for Chronic Obstructive Lung Disease (GOLD) has defined chronic obstructive pulmonary disease (COPD) as a common preventable and treatable disease characterized by persistent airflow limitation, which is usually progressive and associated with an enhanced chronic inflammatory response in the airways and the lung to noxious particles or gases.³¹ Nowadays, COPD is considered a serious global health problem. Its prevalence is estimated at 9-10% for adults aging 40 years or older and is expected to be the third most common cause of death in 2020.^{10,26} The chronic airflow limitation characteristic of COPD is caused by a mixture of small airway disease (obstructive bronchiolitis) and parenchymal destruction (emphysema).²⁶ Moreover, it has been shown that COPD patients with emphysema (confirmed through high resolution computed tomography) have more severe airflow limitation.⁴ Emphysema is defined as the abnormal permanent enlargement of the airspaces distal to the terminal bronchioles, accompanied by destruction of their walls and without obvious fibrosis.^{1,29} Histological *ex vivo* analysis of lungs is performed in order to elucidate the pathophysiology of COPD. In this context, quantitative assessment of emphysematous lesions is required to determine the stage of COPD as well as to evaluate the benefit derived from experimental therapeutic approaches.

Several metrics have been previously defined for emphysema characterization in histological lung section images. In this context, stereological techniques enable to evaluate 3D attributes of the lung like the number of alveoli, the average thickness of the septa or the alveolar surface from a series of sections.¹⁸ These techniques consist in assessing the interaction between the lung section image and a geometric probe (points, lines, planes or volumes).^{11,20} The mean linear intercept (L_m), which estimates the volume-to-surface ratio of the airspaces, has been widely employed in stereological analysis of the lung.⁸ The computation of L_m is based on sampling air segments delimited by alveolar tissue from the image of the lung lobe. Hence, the

value of L_m is calculated as the mean length of the extracted air segments.¹⁴ Although L_m was not conceived as a measure of particle size, it has been employed for the quantitative evaluation of airspace enlargement in emphysema analysis. Recent studies pointed out two main drawbacks of L_m when applied for this purpose.^{12,22} First, L_m depends on the shape of the airspaces. As a result, even if similar sized airspaces are found in distinct lung tissue images, the value of L_m could vary because of their different shapes. In addition, as a measure of the central tendency of a distribution, L_m has shown to underestimate airspace enlargement in mild emphysematous regions characterized by a heterogeneous distribution of the airspaces (i.e., regions with a few enlarged airspaces surrounded by smaller ones). To overcome these limitations, Parameswaran *et al.*²² suggested the use of the equivalent diameter variable (d) of a given airspace. The variable d is defined as the diameter of the circle with an area equal to the underlying airspace. This circumvents the dependence on its shape. A family of indexes derived from the statistical moments of d was proposed as measures of the airspace enlargement associated with emphysematous lesions. Among them, the index D_2 , which takes into account the skewness of d , has shown to be more reliable than the others since it enables the identification of mild emphysema.¹² Indeed, D_2 has been used as the gold-standard metric for airspace enlargement quantification in the study of gas flow inside the lung tissue¹⁵ or in the development of novel *in vivo* techniques of emphysema analysis based on microcomputed tomography (micro-CT).^{2,19}

The analysis of parenchymal tissue sections using D_2 indicates that larger values of this parameter are expected for those areas showing an increased enlargement of the airspaces as a consequence of emphysematous lesions.²² However, while the value of D_2 provides a measure of airspace enlargement, it does not reflect emphysema severity in a given lung area. Recent results demonstrated the utility of D_2 in the classification of healthy and emphysematous lung patches observed through a microscope.^{12,22} According to this approach, a binary identification of parenchymal

tissue can be obtained. Nevertheless, finer resolution in the assessment of emphysema severity would be desired.

In our study, we propose a method to objectively rank the degree of emphysema severity in a lung area from its corresponding D_2 value. To achieve this, a severity index variable (SI), which represents the probability for the lung area under analysis to be emphysematous, is defined. Thus, the rank of severity expressed by means of SI would vary from zero to one, so that lung areas showing more relevant lesions would be associated with values near 1, areas of normal tissue would yield probabilities close to 0 and areas including mild lesions would reflect intermediate probability values. A Bayesian approach was adopted to define the expression of the function that maps the variable D_2 onto the target SI . For this purpose, the statistical distribution of D_2 for normal and emphysematous lung patches was approximated using kernel density estimation techniques. Furthermore, a procedure for the segmentation of the lung section image was designed in order to implement a computer assisted diagnosis tool for histological analysis of these images. The final result is the emphysema severity map for a given lung section. Such a map is intended to help specialists in the quantification and localization of airspace enlargement resulted from emphysema.

2 Materials and methods

2.1 Animal preparation and image acquisition

All experimental protocols involving animal manipulation were approved by the University of Navarra experimentation ethics committee. Sixty A/J male mice, 11 weeks old, were equally distributed into control and treatment groups. Treated mice were intratracheally instilled with 6 units per 30 g of porcine pancreatic elastase (PPE, EC134GI, EPC, MI, USA), as described in a previously published protocol.¹⁶ Control animals were instilled with a saline solution. Five treated mice and five control mice were then sampled 1, 6, 12, 24 hours, 7 and 17 days after elastase administra-

tion. For the present study, a subset of them composed of four control mice, three mice induced with mild emphysematous lesions (24 hours after treatment) and four mice induced with severe emphysematous lesions (17 days after treatment) were randomly selected. Their lungs were collected for histological analysis.

The lungs were fixed at a constant pressure of 20 cm H₂O and three paraffin blocks were made from each mouse. One block with the two halves of the left lung lobe, another block with superior and middle lobes, and the third block with inferior and post-caval lobes. For each block, three non-consecutive sections were cut and stained with hematoxylin and eosin (H&E), yielding a total of nine slides for each mouse. The microtome was used to reach the interior part of the lung. Then, a section was obtained and placed on a slide. For the next section, a displacement of approximately 20-30 μ m along the tissue was used. In the present study, six sections were randomly selected from the nine samples initially obtained for each mouse, resulting in a dataset with 66 lung sections. Whole-slide views of the sections were captured using an automated Axioplan 2ie Zeiss microscope (Carl Zeiss, Jena, Germany). Each slide was initially acquired with a Plan-Neofluar objective (numerical aperture NA = 0.035, magnification 1.25x, pixel resolution 3.546 μ m/pixel). The automatic threshold method proposed by Otsu²¹ was then applied to detect all tissue areas. The size of the objects was measured and only objects with a reasonable size to represent entire sections of lung lobes were considered for further processing. For each object, a bounding box was created and the coordinates of its four vertices were sent to the microscope. Then, tissue areas were automatically scanned at higher magnification with a Plan-Neofluar objective (NA = 0.3, 10x, 0.725 μ m/pixel). Some overlap was allowed between image fields to facilitate the creation of large image mosaics using the Stitcher ImageJ plugin.²⁵ The resulting mosaics were stored in a server for offline quantitative analysis. Figure 1 shows a section from a treated mouse in which the regions including emphysematous lesions have been manually annotated. Additionally,

one healthy lung area and two areas with emphysema are shown at high magnification for comparison.

INSERT FIGURE 1 AROUND HERE

For the development and validation of the index for emphysema severity quantification proposed in our study, the initial group of mice was divided into training and test sets. The former was composed of the 12 lung section images corresponding to one control mouse and one mouse induced with severe emphysematous lesions (6 sections from each of them). This training set was allocated for design and optimization purposes. The lung section images from the nine remaining mice were used for testing the behaviour of our emphysema severity index. The test set was then composed of 54 lung section images, with 6 sections per mouse.

2.2 Emphysema severity index

To quantify the degree of emphysema severity, we defined the severity index (SI) of a specific lung area as the probability that it contains emphysematous lesions. It is worth noting that, according to this definition, emphysema severity and airspace enlargement represent different properties. Nevertheless, they are related to each other since emphysematous lesions are characterized by enlarged airspaces resulting from the destruction of parenchymal tissue.¹ Thus, the emphysema severity index SI presented in our study was expressed in terms of the well-known parameter D_2 , which has shown to be a robust descriptor of pulmonary airspace enlargement.^{12,22} Therefore, given an area of lung tissue, the first step to rank emphysema severity by means of SI is the computation of D_2 . For this purpose, an automated procedure similar to that described by Muñoz-Barrutia *et al.*¹⁹ was applied to obtain D_2 from the image of a lung area. It encompasses the following operations:

1. The 8-bit grayscale green channel is extracted from the 24-bit RGB image containing the lung area since it provides the greatest contrast between the background and the red-blue H&E stained tissue.^{12,19}
2. The image is binarized using the Otsu's method in order to separate the parenchymal tissue from the airspaces.²¹
3. Tissue structures are enhanced by eroding the binary image.
4. The white regions enclosed by the lung tissue represent the airspaces. The area (A) of each of these regions is approximated as its number of pixels. Area values are transformed to equivalent diameter d samples by means of the operation $d = 2\sqrt{\frac{A}{\pi}}$.
5. From the set of samples of the variable d , an estimation of the parameter D_2 is obtained by following the definition provided by Parameswaran *et al.*:²²

$$D_2 = \mu_d \left[1 + \frac{\sigma_d^2}{\mu_d^2 + \sigma_d^2} \left(2 + \frac{\sigma_d \gamma_d}{\mu_d} \right) \right] \quad (1)$$

where μ_d , σ_d^2 and γ_d are the mean, variance and skewness of the variable d , respectively.

As can be observed, the preparation of the image aims to enhance the definition of tissue structures in order to obtain a clear representation of the airspaces of interest. This step involves the modification of the pixels in the original image through operations like thresholding and erosion/dilation.⁹ However, image preprocessing is required to perform automatic analysis of histological lung section images.^{24,27}

Once D_2 has been computed, the aim is to find the mapping function $SI = SI(D_2)$ that provides the corresponding SI . As previously mentioned, the value of SI was modeled as the probability for the lung patch associated with the observed D_2 to be emphysematous. Hence, the target function should meet the three following attributes:

- To represent a probability, the SI must range between zero and one.

- Given two lung patches characterized by $D_2^{(1)}$ and $D_2^{(2)}$ with $D_2^{(1)} \geq D_2^{(2)}$, the values of emphysema severity must reflect this condition by assigning SI values such that $SI^{(1)} \geq SI^{(2)}$. In other words, the function must show a monotonically growing behavior as increased severity must be assigned to larger D_2 values.
- The function $SI = SI(D_2)$ must present a smooth continuous evolution along its domain of definition. This requirement prevents the occurrence of abrupt changes of the function profile, which would be associated with large differences in the SI assigned to similar D_2 samples.

A stochastic approach was adopted for the definition of the function relating D_2 to SI . Hence, both metrics or indexes were treated as random variables. The cumulative distribution function (CDF) of D_2 , which is denoted by F_{D_2} , is suggested as the target mapping function between both variables. According to the inherent attributes of a CDF, F_{D_2} displays the two first properties initially imposed as it monotonically grows between zero and one.³ The third required property is given by the continuous nature of the variable D_2 as only discrete variables would be associated with discontinuities in the CDF. Therefore, we define SI as:

$$SI = F_{D_2}(d_2) = P(D_2 \leq d_2) \quad (2)$$

where d_2 represents a specific realization of the variable D_2 and $P(\cdot)$ denotes the probability of an event. The Bayesian framework was adopted to infer the expression of F_{D_2} from the prior knowledge about the problem.

Initially, it is assumed that this knowledge is given by regions of healthy and emphysematous tissue delimited by a specialist in a lung section image, as depicted in Figure 1. It is worth noting that the specialist is only asked to determine regions with emphysematous lesions but no information on their severity is required. From these regions, a set of control (C) and emphysematous (E) tissue samples of size $W \times W$ pixels are extracted. The value of D_2 for these samples is then obtained following the

procedure described before. As a result, a set of D_2 samples grouped into C and E categories is available. It describes the statistical properties of the proposed problem and will be used to estimate the function F_{D_2} . To this end, according to the total probability theorem, the probability density function (PDF) of the variable D_2 , which is the derivative of F_{D_2} and is termed as f_{D_2} , can be expressed as:³

$$f_{D_2}(d_2) = P(C) f_{D_2|C} + P(E) f_{D_2|E} \quad (3)$$

where $f_{D_2|C}$ and $f_{D_2|E}$ denote the conditional PDF of the variable D_2 in C and E groups, respectively. In addition, $P(C)$ and $P(E)$ are the prior probability of observing a control and an emphysematous lung patch, respectively. The value of SI can be directly obtained from the PDF of D_2 :

$$SI = P(D_2 \leq d_2) = \int_{-\infty}^{d_2} f_{D_2}(\tau) d\tau \quad (4)$$

In practice, the PDF of D_2 is unknown and must be approximated from the available sample set. For this purpose, we used the conventional kernel (Parzen) density estimation procedure.³ Consider a univariate variable X , for which a finite set of N samples is observed. Using the Parzen's method, an approximation to its PDF, which is denoted by f_X , would be obtained as:

$$f_X(x) \approx \frac{1}{N} \sum_{i=1}^N K(x - x_i, h) \quad (5)$$

where $K(\cdot)$ denotes the kernel function and h is its width parameter. Usually, the Gaussian kernel is adopted since it provides smooth approximations to the objective PDF.³ In this case, the kernel would be given by:

$$K(x - x_i, h) = \frac{1}{h\sqrt{2\pi}} \exp \frac{-(x - x_i)^2}{2h^2} \quad (6)$$

The rule proposed by Silverman enables the adjustment of the width parameter h (the standard deviation of the Gaussian), which would be obtained as:²⁸

$$h = \hat{\sigma}_X \left(\frac{4}{3N} \right)^{\left(\frac{1}{5}\right)} \quad (7)$$

where $\hat{\sigma}_X$ is the estimate of the standard deviation of X computed from the initial set of N samples.

This procedure can be applied to the estimation of $f_{D_2|C}$ and $f_{D_2|E}$, which, according to (3) and (4), lead to a manageable expression of the target mapping function $SI = SI(D_2)$.

2.3 Emphysema map

The defined SI function enables the derivation of an emphysema severity map from a given lung lobe section. This map is intended as a tool to facilitate the identification of highly probable emphysematous lung regions. The estimation of an emphysema map involves two main tasks: i) the segmentation of the lung image in order to identify parenchyma pixels and ii) the computation of the SI on each of these pixels.

Image segmentation requires the identification of the lung border along with artifacts due to airways and blood vessels crossing the lung parenchyma, which could be confused with airspaces and must be therefore excluded from further analysis. The key feature exploited for the detection of the lung border was the increased area of the region surrounding the lung compared with the airspaces of interest. To perform border detection, the original lung image is initially converted into a binary image by retaining the green channel and applying the Otsu's method, as previously described for the estimation of D_2 from a lung patch. Subsequently, the following operations are performed (see Figure 2.a):

1. The binary image is eroded in order to enhance the tissue structures in the lung.

2. The resulting holes inside the lung are filled.
3. The biggest foreground (black) area in the image is retained. This operation discards small foreground objects outside the lung. Subsequently, the image is inverted to assign parenchyma pixels a non-zero value.
4. Morphological closing is then applied to smooth out the lung border and recover its original size.

On the other hand, artifacts corresponding to airways and blood vessels are usually surrounded by a border that is thicker than that of the parenchymal tissue that surrounds the airspaces. Therefore, artifact rejection was based on the identification of abnormally thick lines in the image.¹⁹ Once one of these thick borders is detected, we took into account that it might define, or not, a closed region. A specific procedure based on the identification of concavities was then designed to fill open regions. The algorithm for airway and vessel rejection takes as the starting point the binary version of the original lung image and is composed of the following steps (see Figures 2.b and 2.c):

1. Thin tissue structures are removed by dilating the binary image.
2. Small foreground objects (area lower than 30x30 pixels) are removed.
3. Morphological opening is performed to remove irregularities in the definition of the detected thick lines.
4. At this point, each of the remaining foreground objects represents a candidate artifact and is separately processed. This analysis aims to fill the region, if needed, that is defined by the detected line:
 - 4.1. The distance transform is computed. As a result, each pixel is assigned the distance from it to the nearest foreground pixel in the image.
 - 4.2. Local maxima are obtained and identified with concavities.

- 4.3. A local maximum is assumed to be in the interior of the region defined by the line when, in the original image, no tissue is found in a radius equal to the value of the distance transform at such local maximum.
- 4.4. For maxima identified as interior points, a disk of radius equal to their corresponding value of the distance transform is placed on each of them to partially fill the region.
- 4.5. Any remaining hole is filled.

INSERT FIGURE 2 AROUND HERE

We found that the method designed for the detection of airways and blood vessels in the lung parenchyma did not produce false positive cases since abnormally thick lines do not correspond to the border of the airspaces. However, our method was capable of identifying most, but not all, of the artifacts in the image because, for some cases, the surrounding border line was not as thick as expected. To remove these undetected objects, the user was required to manually mark one point inside them. These points were stored and a region growing approach was used to segment out every undetected artifact.

As a result of the image segmentation process, a binary mask indicating those pixels in the parenchyma is obtained. This mask is used to perform the second task in the computation of the emphysema severity map. It involves the following operations from the binary version of the whole lung image:

1. The mask is applied to the binary image of the lung section by means of pixel-by-pixel product.
2. Parenchymal tissue is enhanced by erosion.
3. A $W \times W$ window is centered on each pixel in the parenchyma and the corresponding value of D_2 is obtained. It must be noted that the mask indicates those pixels where the map must be computed and prevents the inclusion of artifacts

as airspaces for the computation of D_2 . Finally, the mapping function is used to assign a SI value to each pixel.

3 Results

3.1 Optimum window size

The optimum window size must be initially determined for the estimation of emphysema maps. The value of W defines the extent of the local region considered around the pixel for which SI is computed. The definition of W reveals a trade-off between the statistical reliability of the obtained D_2/SI and the spatial resolution of the severity map. For an increased value of W , a higher number of samples of the variable D_2 will be obtained, as it is expected that more airspaces will be included in the analysis, leading to a more reliable estimation of D_2/SI . However, a large W is associated with lower spatial accuracy in the assignment of SI to the lung pixels. Since a larger area of the lung is considered, the unique correspondence between the central pixel of the $W \times W$ window and the obtained D_2/SI value is lost.

To determine the optimum window size, we evaluated the ability of D_2 to characterize lung tissue samples as a function of W . To this end, we selected pixels from regions of healthy and emphysematous tissue initially annotated by a specialist on the original lung section image. A $W \times W$ window was then centered on each of these pixels to define control (C) and emphysematous (E) patches for which D_2 was computed. To assess the reliability of the estimated D_2 , its performance in the identification of patches from both C and E categories was analyzed. The performance measures adopted for this purpose were the area under the receiver operating characteristic curve (AUC)⁵ and the p -value derived from the non-parametric Kruskal-Wallis test.¹³ Both measures were computed for different values of W , which was varied between $W_{min} = 11$ and $W_{max} = 1001$ (an odd value was used for the window size to unambiguously identify the central pixel). In our experiment, a total of 283

pixels (123 from healthy tissue regions and 160 from emphysematous ones) were selected on the 12 lung sections in the training set. The evolution of the AUC and the p -value achieved by the variable D_2 as a function of W is depicted in Figure 3. As expected, the capability of D_2 to characterize emphysema grows as W is increased. Nevertheless, it must be noted that beyond certain value of W ($W = 751$ pixels) the classification utility of D_2 is not further improved. Therefore, the optimum value of W was set to 751 pixels.

INSERT FIGURE 3 AROUND HERE

3.2 Mapping function

According to the optimum window size, a new set of 399 patches of size 751×751 pixels (190 control and 209 emphysematous samples) was extracted from the training lung sections. As detailed in the proposed methodology, this training set was used to infer the expression of the conditional PDF of D_2 in C and E categories, which lead to the definition of the function $SI = SI(D_2)$.

The Parzen window method was applied to estimate $f_{D_2|C}$ and $f_{D_2|E}$ as expressed in (5). Equal prior probability was assumed for healthy and emphysematous patches, i.e., $P(C) = P(E) = 0.5$. The obtained functions are depicted in Figure 4 together with the SI function, which is given by (3) and (4). The result reveals the differences between the distributions of D_2 for C and E categories. Emphysematous lung patches are associated with higher values of D_2 (airspace enlargement), which are concentrated in a wider range. The approximated density functions $f_{D_2|C}$ and $f_{D_2|E}$ can be used to estimate the probability of error in the identification of lung patches from both

categories according to the value of D_2 . Using a Bayesian approach, this probability would be obtained as $P(C)p(D_2 \geq u|C) + p(E)p(D_2 \leq u|E)$, where u determines the optimum decision threshold given by the intersection point between both curves.³

From our data, the value of u was found to be $114.38 \mu\text{m}$ and the probability of error

was estimated as 2.93%. This result shows the utility of D_2 to perform binary classification of lung patches as healthy or emphysematous, as reported in previous studies.¹² Finally, it must be appreciated that the obtained SI function given by F_{D_2} reflects the three properties initially required since it maps the whole domain of D_2 onto the 0-1 interval, has a monotonically growing behaviour and reflects a smooth profile.

INSERT FIGURE 4 AROUND HERE

3.3 Emphysema maps

The segmentation procedure described before was used to obtain the masks of the 54 lung sections in the test set. Subsequently, the resulting SI function was applied to each of them for the computation of their respective emphysema maps. Severity maps provide the probability for each pixel in the lung parenchyma to fall in an emphysematous region. To analyze the differences between the maps from normal untreated mice, mice induced with mild emphysema (treated for 24 hours) and mice induced with severe emphysema (treated for 17 days), we calculated the distribution of SI for the lung sections in these three groups, as depicted in Figure 5.

INSERT FIGURE 5 AROUND HERE

The figure reveals differences in the statistical distribution of SI in each of the severity groups. For sections from normal mice, a higher proportion of the SI values in the map were in the interval between 0 and 0.5. In contrast, in the case of sections from mice induced with mild and severe emphysema, map pixels were concentrated on SI values between 0.5 and 1. In addition, a different behaviour was observed between these two groups. Lung sections from mice induced with mild emphysema exhibited a higher concentration of map pixels in the interval between 0.5 and 0.7, approximately. Sections from mice induced with severe emphysema tended to yield a higher proportion of SI values between 0.7 and 1. From this analysis, the domain of

the variable SI can thus be divided into three bands or intervals related to the severity of the emphysematous lesions:

- Normal band ($0 \leq SI < 0.5$). SI values in this band indicate normal tissue. They are more probable in sections from normal mice than in those from mice induced with mild and severe emphysema.
- Mild band ($0.5 \leq SI \leq 0.7$). SI values in this band indicate mild emphysematous lesions. They are more probable in sections from mice induced with mild emphysema than in those from normal mice and mice induced with severe emphysema.
- Severe band ($0.7 < SI \leq 1$). SI values in this band indicate severe emphysematous lesions. They are more probable in sections from mice induced with severe emphysema than in those from normal mice and mice induced with mild emphysema.

We define the parameters A_{norm} , A_{mild} and A_{sev} as a set of quantitative descriptors of emphysema from a lung section. They account for the percentage of SI points in the emphysema map that fall in normal, mild and severe bands, respectively. We evaluated the utility of these descriptors for the characterization of emphysema severity in a lung section. For comparison purposes, conventional metrics L_m and D_2 were also assessed. For a given section, L_m and D_2 were estimated by randomly selecting a total of 25 lung patches in which airways and blood vessels were avoided, as described by Jacob et al.¹² The samples of the intercept length (L) and the equivalent diameter (d) from all the patches in a lung section were assembled into a single dataset.¹² Then, L_m and D_2 were computed from the set of L and d samples, respectively. To extract samples of the variable L , the direct method for L_m estimation described by Knudsen et al.¹⁴ was applied. Figure 6 shows the boxplots of the five evaluated lung parameters in each of the three severity groups: normal, mild emphysema and severe emphysema. It can be observed that each of the parameters can easily distinguish normal sections from those with mild and severe emphysematous lesions.

Nevertheless, as reflected by the boxplots, the most difficult task is the discrimination between the two latter groups. The Kruskal-Wallis method was used to test the statistical significance of the differences exhibited by each parameter between lung sections from normal mice, mice induced with mild emphysema and mice induced with severe severe emphysema.¹³ The p -value for each pair of severity groups is summarized in Table 1. The results reveal that A_{mild} is the most effective descriptor of the degree of emphysema severity in a lung section since we found statistically significant differences (p -value < 0.001) between the three groups. Additionally, although other parameters like L_m , D_2 and A_{sev} did not yield significant differences between mild and severe emphysematous sections, they showed a distinct trend in the values assigned to samples from both groups as reflected by the gap between the means in these groups. Hence, higher values are expected for these parameters in the case of lung sections from mice induced with severe lesions. Note that, even though L_m has been proved to fail in the identification of emphysematous lung patches with a heterogeneous distribution of the airspaces,^{12,22} it showed an acceptable capability to characterize emphysema severity for a whole lung section, yielding similar or smaller p -values than D_2 . As highlighted by Weibel,³² L_m is computed as the central tendency of the intercept length and, thus, it cannot reflect the variability observed in lung patches with many small airspaces and a few large ones. Tissue areas with such a heterogeneous distribution are localized in specific regions of the lung corresponding to the transition from normal to emphysematous tissue, i.e., they represent a small percentage of the total lung section. Therefore, as the computation of L_m and D_2 was based on the random selection of a set of lung patches, the probability of sampling areas with a high variability in the size of the airspaces will be small, having no relevant influence on the final estimate of these parameters.

INSERT TABLE 1 AROUND HERE

INSERT FIGURE 6 AROUND HERE

The statistical test indicates that the evaluated parameters may contain different information on the severity of the emphysematous lesions in a lung section. To study this hypothesis, multivariate analysis based on the combination of the five parameters was conducted. We used the Fisher's linear discriminant (FLD) method to visualize the multivariate patterns extracted from each lung section image in normal, mild and severe groups.⁷ A transformation matrix T_{FLD} , which maps input patterns onto a two-dimensional space, is defined by maximizing the ratio of the inter-class variability to the intra-class variability for the transformed samples. Figure 7 depicts the projection of the patterns on the two FLD components, which have been denoted as FLD_1 and FLD_2 . A different trend can be observed for patterns in each of the three severity groups, revealing the diagnostic utility of the combination of uncorrelated variables. On the one hand, the component FLD_1 allows us to discriminate normal sections from those corresponding to treated mice induced with mild and severe emphysema. On the other hand, FLD_2 captures the differences between sections in mild and severe groups. Furthermore, a higher degree of variability is observed in lung sections from severe mice since the corresponding cluster is characterized by a larger size. This suggests that a wider range of tissue states can be found in the parenchyma of mice exposed to the effects of treatment for a longer period of time, varying from normal tissue to severe lesions. Our result indicates that the simultaneous analysis of several parameters enables a more accurate characterization of emphysema, which is in agreement with the recommendation made by Mühlfeld and Ochs.¹⁸

INSERT FIGURE 7 AROUND HERE

Finally, as an example, Figure 8 shows the maps obtained for three sections corresponding to a normal mouse, a mouse induced with mild emphysema and a mouse induced with severe emphysema, respectively. Lung areas identified as normal, mild and severe were automatically obtained by selecting map pixels with an SI in the corresponding band. As can be observed, most of the lung section from the normal

mouse was quantified with small SI values indicating a lower probability of emphysema. Additionally, an interesting point here is the differences between the maps of the two treated mice. For the mouse induced with mild emphysema, a higher proportion of the lung section is assigned with intermediate SI values, reflecting the predominance of mild emphysematous lesions. For the mouse exposed to treatment during a longer period, a relevant percentage of the lung section has been given increased values of SI . This reflects that, in addition to mild emphysema, severe lesions have been developed in most of the parenchyma. Therefore, the obtained maps show a coherent behaviour of the proposed index SI .

INSERT FIGURE 8 AROUND HERE

4 Discussion and conclusions

Emphysema commonly manifests as a component of COPD. Animal models provide a useful means to study this disease and test the efficacy of drugs. In this research, we address the problem of quantifying emphysema severity in histological lung sections. For this purpose, we defined the emphysema severity index (SI), which provides the probability for an observed lung area to be emphysematous. The variable SI was expressed as a function of D_2 , which effectively quantifies airspace enlargement in the lung, by means of the CDF of the latter. A kernel-based approach was applied to estimate the statistical distribution of D_2 for both control and emphysematous patches in order to obtain the expression of the $SI = SI(D_2)$ function. Finally, we evaluated the utility of this function by calculating the emphysema severity map of a lung section, enabling the localization of areas affected by emphysematous lesions.

We present two main contributions to the *ex vivo* histological analysis of lung sections in the context of emphysema and COPD research: the definition of the SI variable and the computation of the emphysema map for a lung section. Our SI is a step forward over currently existing metrics such as L_m and D_2 for the quantification

of airspace enlargement due to emphysema. These metrics enable a relative evaluation on the extent of emphysema by assuming increased severity for lung areas with larger values of L_m/D_2 with respect to those with smaller ones. Hence, L_m and D_2 have been traditionally adopted as a reference in previous studies on emphysema and COPD involving animal models.^{15,24,27} However, a scale of severity had not been established for these metrics. This gap between airspace enlargement quantification and the degree of emphysema severity is overcome by the definition of the SI function, which provides a novel analytical expression for the interpretation of D_2 .

On the other hand, emphysema maps provide spatial information on the progression of the lesions. Usually, the characterization of emphysema in lung section images has been carried out by means of stereological techniques such as the intercept length or the disector. These techniques typically yield a number that quantifies a specific lung attribute related to the alveolar wall destruction or the airspace enlargement.¹⁸ For example, the latter has been widely evaluated using L_m , which is estimated from a set of tissue patches extracted from the underlying lung section image. Peces-Barba *et al.*²⁴ used a minimum of 27 patches from each section while Rangasamy *et al.*²⁷ extracted 15 patches. In contrast, for the computation of emphysema maps, every pixel in the lung image is assigned its corresponding SI value. The information contained in the map can thus be employed for different purposes. Hence, it enables the spatial localization of lung areas characterized by a higher emphysema severity, as shown in the example of the Figure 8. In addition, new emphysema descriptors such as A_{norm} , A_{mild} and A_{sev} can be defined. As reflected by our results, A_{mild} summarizes the information in the lung image, providing an objective quantification of the damage caused by emphysema.

It is worth noting that the proposed emphysema maps are not presented as an alternative to the currently existing metrics for emphysema quantification used in histology. These maps are intended to provide additional information for the specialist in the field. As indicated by Mühlfeld and Ochs,¹⁸ a combination of several param-

eters may be the most effective approach to characterize parenchyma destruction in emphysema. Our experiments show that the suggested map features A_{norm} , A_{mild} and A_{sev} can be used together with other measurements towards a more efficient description of emphysematous lesions. In this vein, morphometry features like geometric attributes of the alveolar septa (volume, surface area and thickness), the volume of alveoli or the number of alveoli could be considered.¹⁸ Furthermore, emphysema maps enable the spatial localization of the emphysematous lesions. This information could be used for the assessment of patterns of tissue destruction in order to explore the relationship between emphysema and the physiological functions of the lung.^{6,23}

To our knowledge, no preceding studies on the computation of emphysema severity maps from histological lung sections have been reported. However, similar approaches have been recently developed on CT images. Castaldi et al.⁶ classified lung patches from the CT image into one of six different emphysema categories: no emphysema, mild, moderate or severe centrilobular emphysema, panlobular emphysema and pleural-based emphysema. They used a grid to divide the whole lung image into square patches. Once these are labeled, an emphysema map of the CT scan is obtained. Sorensen et al.³⁰ suggested a similar methodology to process CT images. Nevertheless, a more simple approach was considered by assuming a single category of centrilobular emphysema. For the comparison of our study with these previous ones, it must be appreciated that histological and CT analyses are intended for distinct purposes. For instance, histological assessment of lung tissue enables the evaluation of treatments and could be used as a reference for quantification techniques based on non-invasive procedures like CT.^{17,19} The main advantage of CT is given by its non-invasive nature, making possible the assessment of living individuals. Yet, the radiation exposure is a clear drawback of this technique. On the other hand, the maps reported by the cited studies are characterized by a reduced resolution in both the spatial coordinate and the emphysema severity scale. It is motivated by the patch-by-patch approach adopted to process the original lung image and the limited number

of labels (categories) considered to rank severity. In contrast, our approach suggests pixel-by-pixel analysis of the lung tissue, providing a continuous value of probability in the 0-1 range to quantify emphysema severity. As a future research line, the application of our methodology to CT lung images should be explored, since it would enable the computation of emphysema maps in humans. These maps could provide a powerful diagnostic tool in the context of emphysema and COPD.

Several limitations can be found in our study. **First, standard sampling approaches** recommended in stereology for unbiased analysis of the lung were not considered.¹¹ The presented results would then be biased in order to provide conclusions about the 3D lung structure, since larger airspaces have a higher probability of being sampled.³² Therefore, appropriate sampling rules described by Hsia et al.¹¹ should be taken into account for an unbiased representation of the whole lung organ by means of the extracted sections. On the other hand, future work will be also focused on the segmentation step. It enables the identification of parenchyma pixels, being a key issue to achieve map representations. A semi-automatic segmentation procedure based on morphological operators was designed, as the user was required to indicate artifacts that were not detected by the algorithm. From our experiments, we estimated that the average time for this manual annotation was approximately 2 minutes. However, segmentation should be independent of the user to achieve fully automatic analysis of a lung section. Finally, the mapping function relating D_2 and SI is influenced by the adopted animal model. Hence, the application to other models would involve the definition of a new training set containing samples of normal and emphysematous tissue in order to infer the statistical properties of D_2 .

In summary, accurate assessment of emphysema severity in histological analysis of lung sections is key for a successful characterization of COPD and treatment strategies in pre-clinical trials. A novel parameter for ranking emphysema severity, the so called emphysema severity index (SI), has been proposed. It has been defined as a function of the airspace enlargement observed in lung tissue, which is quantified

by D_2 . Additionally, a semi-automatic procedure has been designed to evaluate the SI for a whole lung section image, resulting in an emphysema severity map. This approach is proposed as an assistant software tool for pathologists and researchers involved in the study of emphysema and COPD.

Acknowledgements

J. Victor Marcos is a research fellow at Institute of Optics (CSIC) under the "Juan de la Cierva" programme funded by the Spanish Ministry of Economy and Competitiveness.

References

- ¹ American Thoracic Society. Definitions, epidemiology, pathophysiology, diagnosis, and staging. *Am. J. Respir. Crit. Care Med.* 152:S78-S83, 1995.
- ² Artachevarria, X., D. Blanco, G. de Biurrun, M. Ceresa, D. Perez-Martin, G. Bastarrika, J.P. de Torres, J.J. Zulueta, L.M. Montuenga, C. Ortiz-de-Solorzano, and A. Muoz-Barrutia. Evaluation of micro-CT for emphysema assessment in mice: comparison with non-radiological techniques. *Eur. Radiol.* 21:954–962, 2011.
- ³ Bishop, C.M. *Neural Networks for Pattern Recognition*. Oxford: Oxford University Press, 1995.
- ⁴ Boschetto, P., M. Miniati, D. Miotto, F. Braccioni, E. De Rosa, I. Bononi, A. Papi, M. Saetta, L.M. Fabbri, and C.E. Mapp. Predominant emphysema phenotype in chronic obstructive pulmonary disease patients. *Eur. Respir. J.* 21:450–454, 2003.
- ⁵ Bradley, A.P. The use of the area under the ROC curve in the evaluation of machine learning algorithms. *Pattern Recogn.* 30:1145–1159, 1997.
- ⁶ Castaldi, P.J., R. San Jose-Estepar, C.S. Mendoza, C.P. Hersh, N. Laird, J.D. Crapo, D.A. Lynch, E.K. Silverman, and G.R. Washko. Distinct quantitative computed tomography emphysema patterns are associated with physiology and function in smokers. *Am. J. Respir. Crit. Care Med.* 188:1083–1090, 2013.
- ⁷ Duda, R.O., P.E. Hart, D.G. Stork. *Pattern classification*. New York: John Wiley & Sons, 2012.
- ⁸ Dunnill, M. S. Quantitative methods in the study of pulmonary pathology. *Thorax* 17:320–328, 1962.
- ⁹ Gonzalez, R.C., R.E. Woods, and S.L. Eddins. *Digital image processing using MATLAB*. New Jersey: Pearson Prentice Hall, 2004.

- ¹⁰ Halbert, R.J., J.L. Natoli, A. Gano, E. Badamgarav, A.S. Buist, and D.M. Mannino. Global burden of COPD: systematic review and meta-analysis. *Eur. Respir. J.* 28:523–532, 2006.
- ¹¹ Hsia, C.C.W., M.H. Dallas, M. Ochs, and E.R. Weibel. An official research policy statement of the American Thoracic Society/European Respiratory Society: standards for quantitative assessment of lung structure. *Am. J. Resp. Crit. Care* 181:394–418, 2010.
- ¹² Jacob, R.E., J.P. Carson, K.M. Gideon, B.G. Amidan, C.L. Smith, and K.M. Lee. Comparison of two quantitative methods of discerning airspace enlargement in smoke-exposed mice. *PloS One* 4: e6670, 2009.
- ¹³ Jobson, J.D. *Applied Multivariate Data Analysis. Volume II: Categorical and Multivariate Methods.* New York: Springer, 1991.
- ¹⁴ Knudsen, L., E.R. Weibel, H.J.G. Gundersen, F.V. Weinstein, and M. Ochs. Assessment of air space size characteristics by intercept (chord) measurement: an accurate and efficient stereological approach. *J. Appl. Physiol.* 108:412–421, 2010.
- ¹⁵ Kyriazis, A., I. Rodriguez, N. Nin, J.L. Izquierdo-Garcia, J.A. Lorente, J.M. Perez-Sanchez, J. Pesic, L.E. Olsson, and J. Ruiz-Cabello. Dynamic ventilation 3He MRI for the quantification of disease in the rat lung. *IEEE Trans. Biomed. Eng.* 59:777–786, 2012.
- ¹⁶ Lakatos, H.F., H.A. Burgess, T.H. Thatcher, M.R. Redonnet, E. Hernady, J.P. Williams, and P.J. Sime. Oropharyngeal aspiration of a silica suspension produces a superior model of silicosis in the mouse when compared to intratracheal instillation. *Exp. Lung Res.* 32:181–199, 2006.
- ¹⁷ Mata, J.F., T.A. Altes, J. Cai, K. Ruppert, W. Mitzner, K.D. Hagspiel, B. Patel, M. Salerno, J.R. Brookeman, E.E. de Lange, W.A. Tobias, H.T.J. Wang, G.D. Cates, and J.P. Mugler. Evaluation of emphysema severity and progression in a rabbit model: comparison of hyperpolarized ³He and ¹²⁹Xe diffusion MRI with lung morphometry. *J. Appl. Physiol.* 102:1273–1280, 2007.
- ¹⁸ Mühlfeld, C., and M. Ochs. Quantitative microscopy of the lung: a problem-based approach. Part 2: stereological parameters and study designs in various diseases of the respiratory tract. *Am. J. Physiol.-Lung Cell. Mol. Physiol.* 305:L205–L221, 2013.
- ¹⁹ Muñoz-Barrutia, A., M. Ceresa, X. Artaechevarria, L.M. Montuenga, and C. Ortiz-de-Solorzano. Quantification of lung damage in an elastase-induced mouse model of emphysema. *J. Biomed. Imaging* 2012:1–11 2012.
- ²⁰ Ochs, M., and C. Mühlfeld. Quantitative microscopy of the lung: a problem-based approach. Part 1: basic principles of lung stereology. *Am. J. Physiol.-Lung Cell. Mol. Physiol.* 305:L15–L22, 2013.
- ²¹ Otsu, N. A threshold selection method from gray-level histograms. *IEEE Trans. Syst., Man Cybern.* 9:62–66, 1979.
- ²² Parameswaran, H., A. Majumdar, S. Ito, A.M. Alencar, and B. Suki. Quantitative characterization of airspace enlargement in emphysema. *J. Appl. Physiol.* 100:186–193, 2006.

- ²³ Parameswaran, H., A. Majumdar, and B. Suki. Linking microscopic spatial patterns of tissue destruction in emphysema to macroscopic decline in stiffness using a 3D computational model. *PLoS Comput. Biol.* 7:e1001125, 2011.
- ²⁴ Peces-Barba, G., J. Ruiz-Cabello, Y. Cremillieux, I. Rodriguez, D. Dupuich, V. Callot, M. Ortega, M.L. Rubio-Arbo, M. Cortijo, and N. Gonzalez-Mangado. Helium-3 MRI diffusion coefficient: correlation to morphometry in a model of mild emphysema. *Eur Respir J* 22:14-19, 2003.
- ²⁵ Preibisch, S., S. Saalfeld, and P. Tomancak. Globally optimal stitching of tiled 3D microscopic image acquisitions. *Bioinformatics* 25:1463–1465, 2009.
- ²⁶ Rabe, K.F., S. Hurd, A. Anzueto, P.J. Barnes, S.A. Buist, P. Calverley, Y. Fukuchi, C. Jenkins, R. Rodriguez-Roisin, C. van Weel, and J. Zielinski. Global strategy for the diagnosis, management, and prevention of chronic obstructive pulmonary disease: GOLD executive summary. *Am. J. Respir. Crit. Care Med.* 176:532–555, 2007.
- ²⁷ Rangasamy, T., C.Y. Cho, R.K. Thimmulappa, L. Zhen, S.S. Srisuma, T.W. Kensler, M. Yamamoto, I. Petrache, R.M. Tuder, and S. Biswal. Genetic ablation of Nrf2 enhances susceptibility to cigarette smoke-induced emphysema in mice. *J. Clin. Invest.* 114:1248–1259, 2004.
- ²⁸ Silverman, B.W. *Density Estimation for Statistics and Data Analysis*. London: Chapman & Hall, 1998.
- ²⁹ Snider, G.L., J. Kleinerman, W. Thurlbeck, and Z. Bengali. The definition of emphysema: report of a national heart, lung and blood institute, division of lung diseases workshop. *Am. Rev. Respir. Dis.* 132:182–185, 1985.
- ³⁰ Sorensen, L., S.B. Shaker, and M. De Bruijne. Quantitative analysis of pulmonary emphysema using local binary patterns. *IEEE Trans. Med. Imag.* 29:559–569, 2010.
- ³¹ Vestbo, J., S.S. Hurd, A.G. Agustí, P.W. Jones, C. Vogelmeier, A. Anzueto, P.J. Barnes, L.M. Fabbri, F.J. Martinez, M. Nishimura, R.A. Stockley, D.D. Sin, and R. Rodriguez-Roisin. Global strategy for the diagnosis, management, and prevention of chronic obstructive pulmonary disease: GOLD executive summary. *Am. J. Respir. Crit. Care Med.* 187:347–365, 2013.
- ³² Weibel, E.R., H. Parameswaran, A. Majumdar, S. Ito, A.M. Alencar, B. Suki, W. Mitzner, C.C.W. Hsia, H. Fehrenbach, J.P. Butler. Morphological quantitation of emphysema: a debate. *J. Appl. Physiol.* 100:1419–1421, 2006.

Tables, figure legends

| | L_m | D_2 | A_{norm} | A_{mild} | A_{sev} |
|------------------|---------|---------|------------|------------|-----------|
| Normal vs Mild | < 0.001 | < 0.001 | < 0.001 | < 0.001 | < 0.001 |
| Normal vs Severe | < 0.001 | < 0.001 | < 0.001 | < 0.001 | < 0.001 |
| Mild vs Severe | 0.0016 | 0.0290 | 0.9748 | < 0.001 | 0.0095 |

Table 1 Assessment of the statistical significance of the differences between severity groups for each of the lung parameters using the non-parametric Kruskal-Wallis test.

Fig. 1 Lung section from a treated mouse with manually annotated emphysematous lesions. Three different patches are highlighted: (a) a lung patch including healthy tissue and (b), (c) two lung patches from the damaged area.

Fig. 2 Segmentation procedure for the identification of lung parenchyma pixels. (a) The detection of the lung border is based on the higher area of the background when compared to the airspaces of interest. (b) Artifacts given by airways and blood vessels are found by detecting thick lines in the region limited by the lung border. (c) If the structure identified as a potential artifact is not perfectly closed, a filling strategy is carried out by detecting the points in the interior of the region.

Fig. 3 Influence of the window size on the classification ability of D_2 . Both the AUC and the p -value are used to assess the differences between C and E lung patches.

Fig. 4 Estimation of the statistical distribution of D_2 from training patches using the kernel density approach: (a) approximated PDF and (b) the corresponding CDF. The latter defines the mapping function from D_2 to SI .

Fig. 5 Statistical analysis of the SI variable from lung section images in the test set. The distribution of this variable in lung sections from normal mice, mice induced with mild emphysema and mice induced with severe emphysema is studied. A characteristic band can be identified for each of these severity groups (dotted lines): normal ($0 \leq SI < 0.5$), mild ($0.5 \leq SI \leq 0.7$) and severe ($0.7 \leq SI \leq 1$).

Fig. 6 Boxplots showing the statistical distribution of the five lung parameters in the three severity groups: normal, mild emphysema and severe emphysema.

Fig. 7 Multivariate characterization of lung sections images. Projection of the multivariate patterns using the transformation matrix obtained from Fisher's linear discriminant (FLD) analysis.

Fig. 8 Emphysema maps for three different lung sections from the test set: (a) lung section from a normal untreated mouse, (b) lung section from a mouse induced with mild emphysema (24 hours after treatment) and (c) lung section from a mouse induced with severe emphysema (17 days after treatment). For each of the sections, three different representations are shown: the original lung section image (left), the obtained emphysema severity map (middle) and lung areas identified as normal ($0 \leq SI < 0.5$), mild ($0.5 \leq SI \leq 0.7$) or severe ($0.7 \leq SI \leq 1$) emphysema (right).

Figure 1
[Click here to download high resolution image](#)

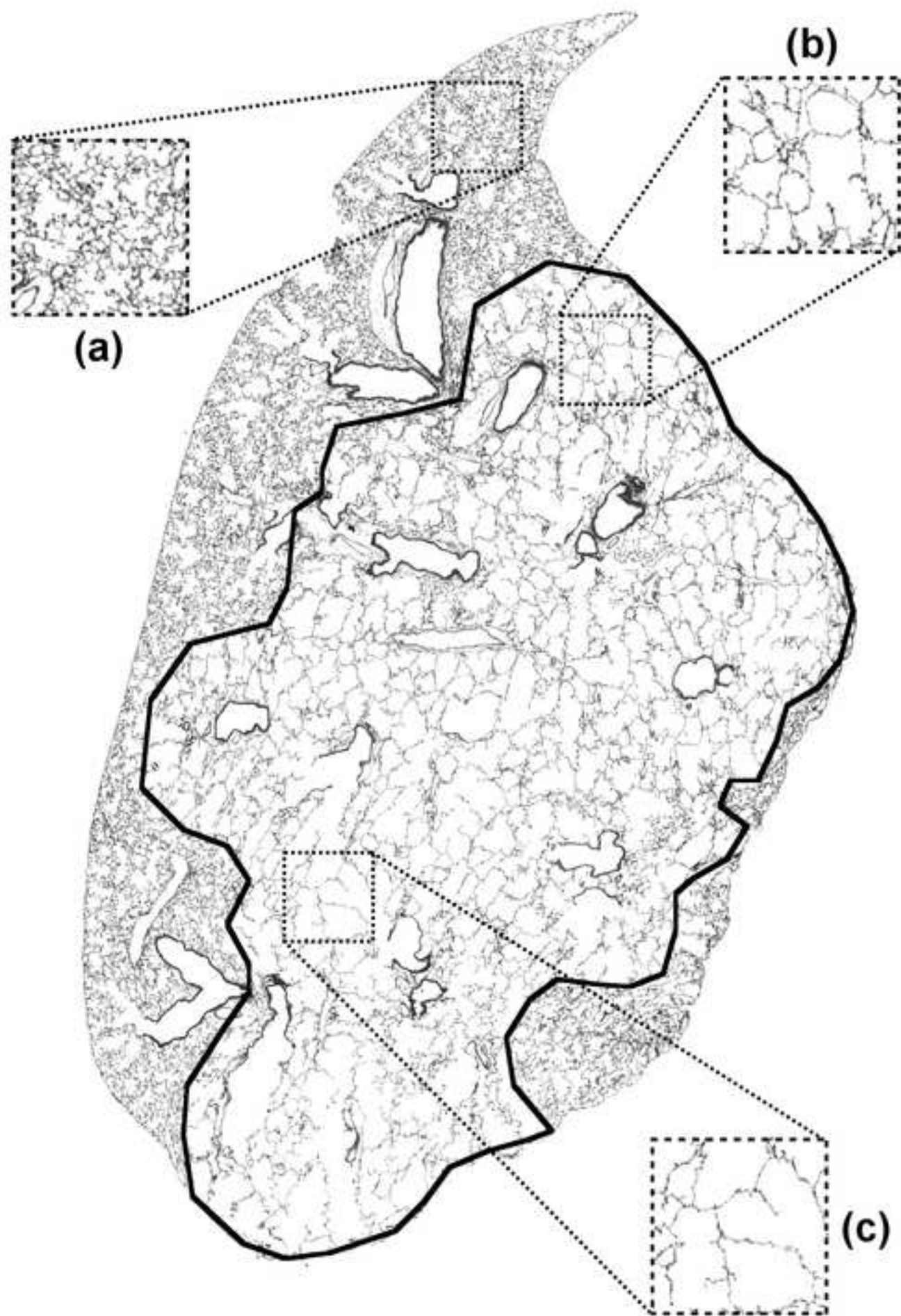
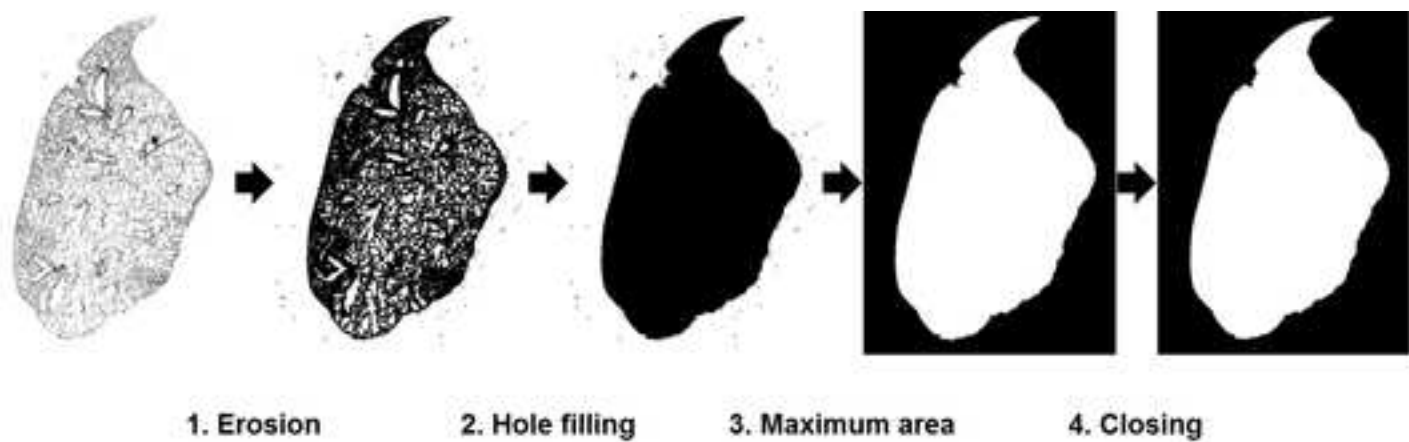
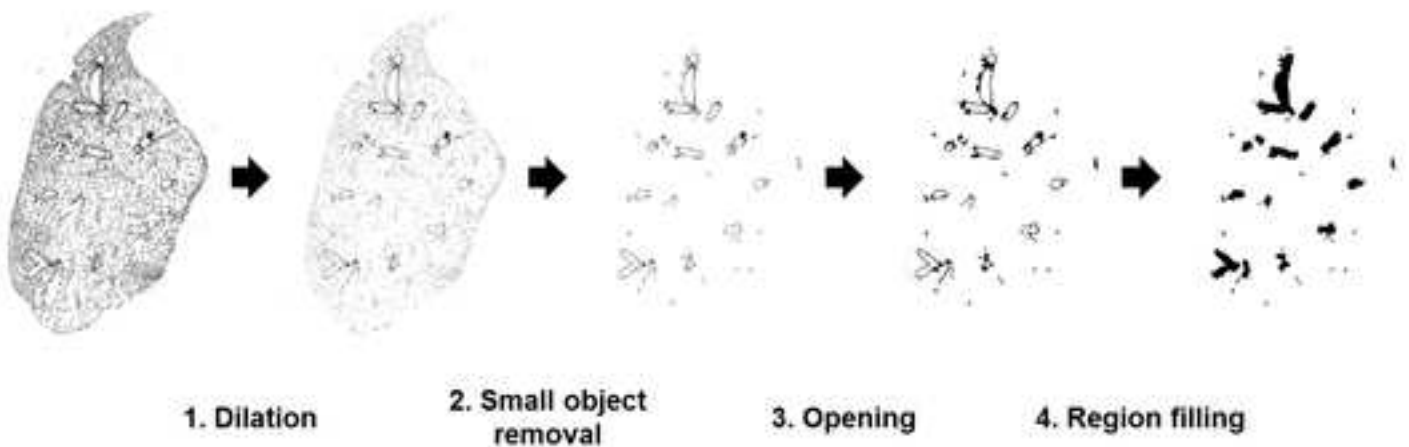


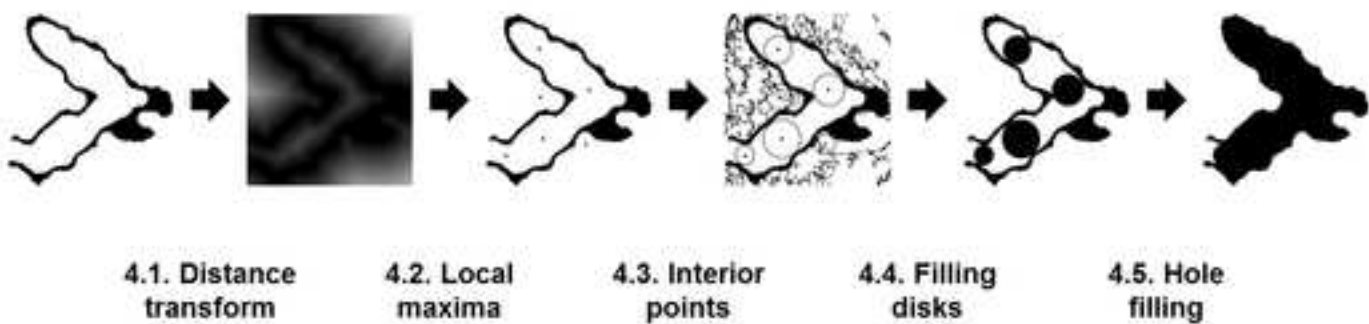
Figure 2
[Click here to download high resolution image](#)



(a)



(b)



(c)

Figure 3
[Click here to download high resolution image](#)

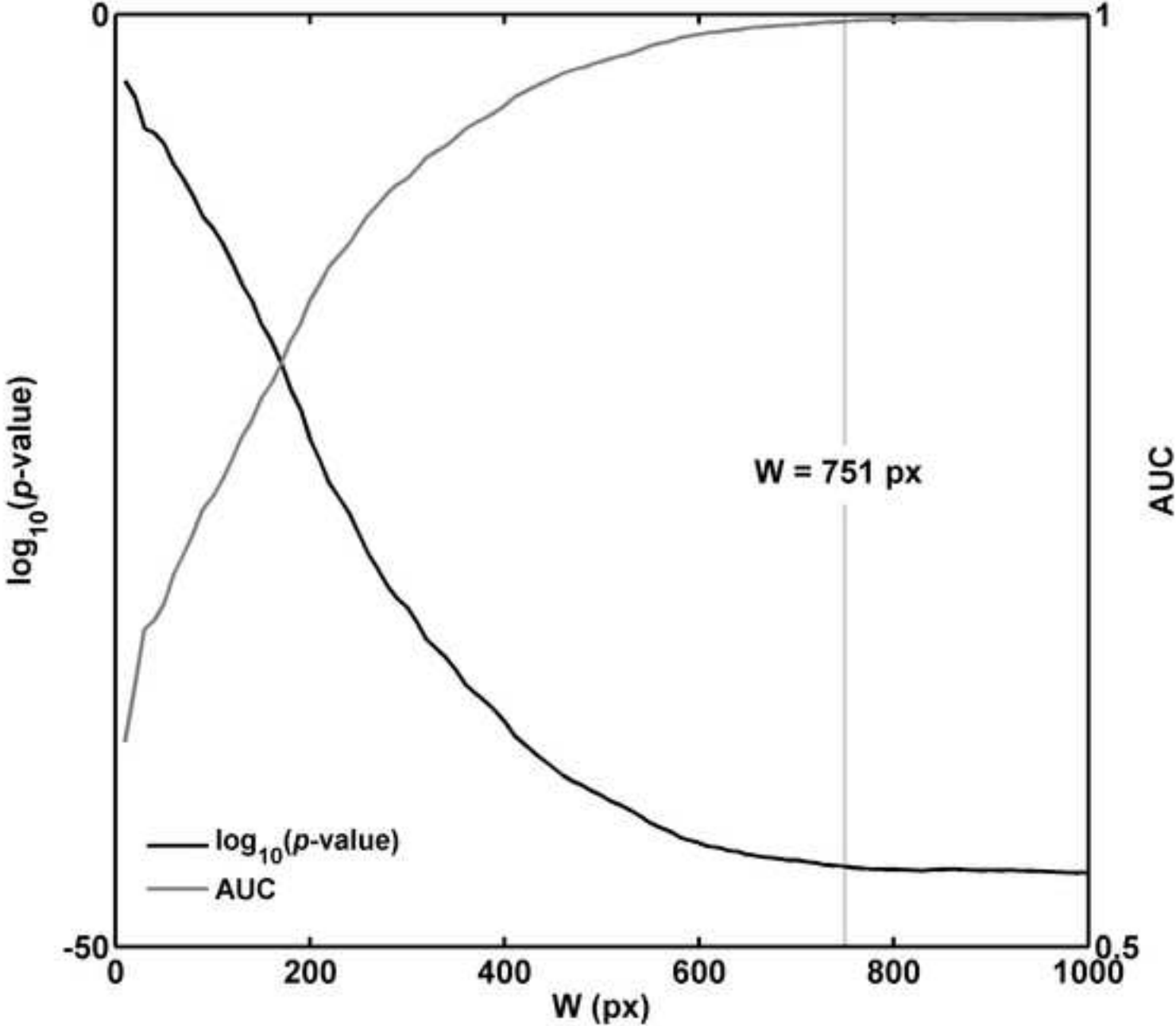


Figure 4
[Click here to download high resolution image](#)

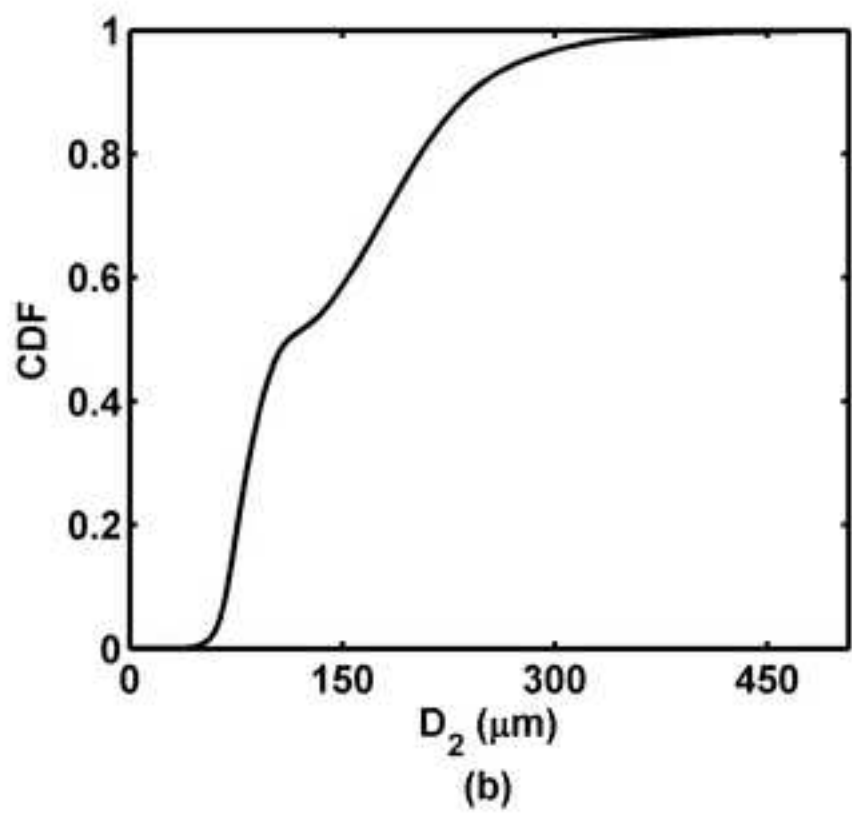
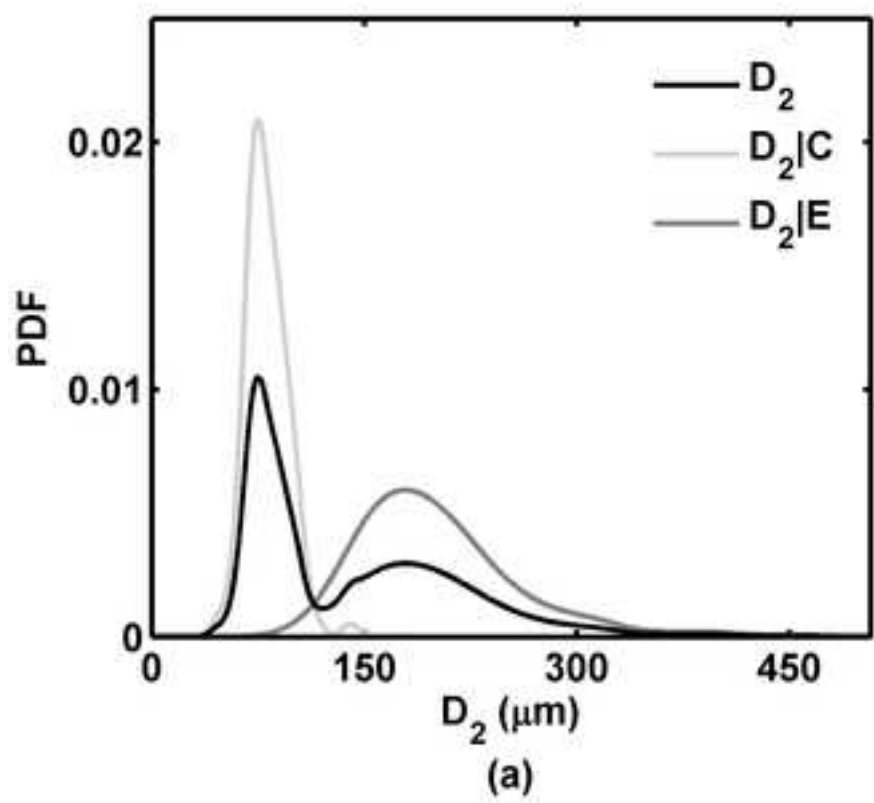


Figure 5
[Click here to download high resolution image](#)

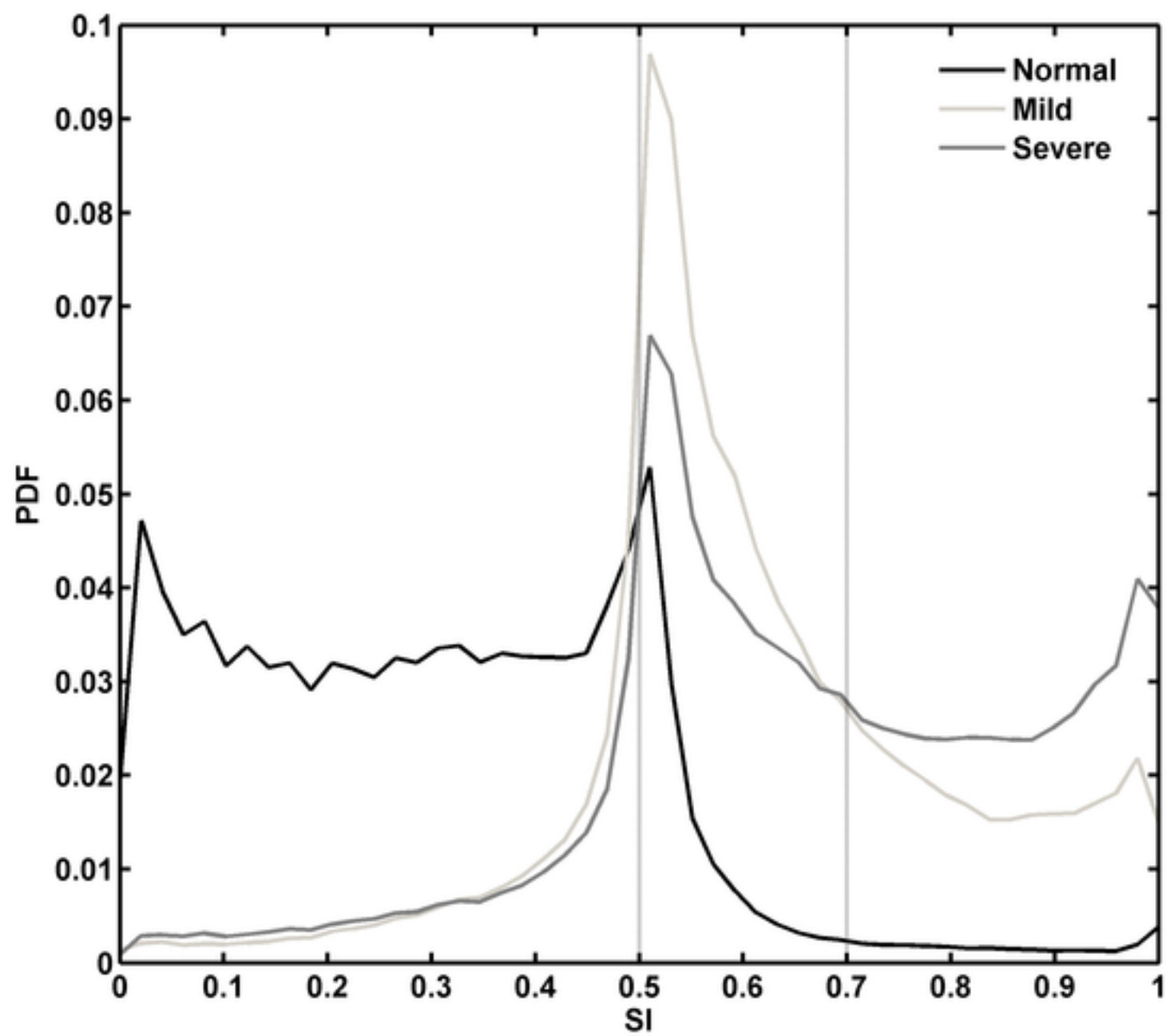


Figure 6
[Click here to download high resolution image](#)

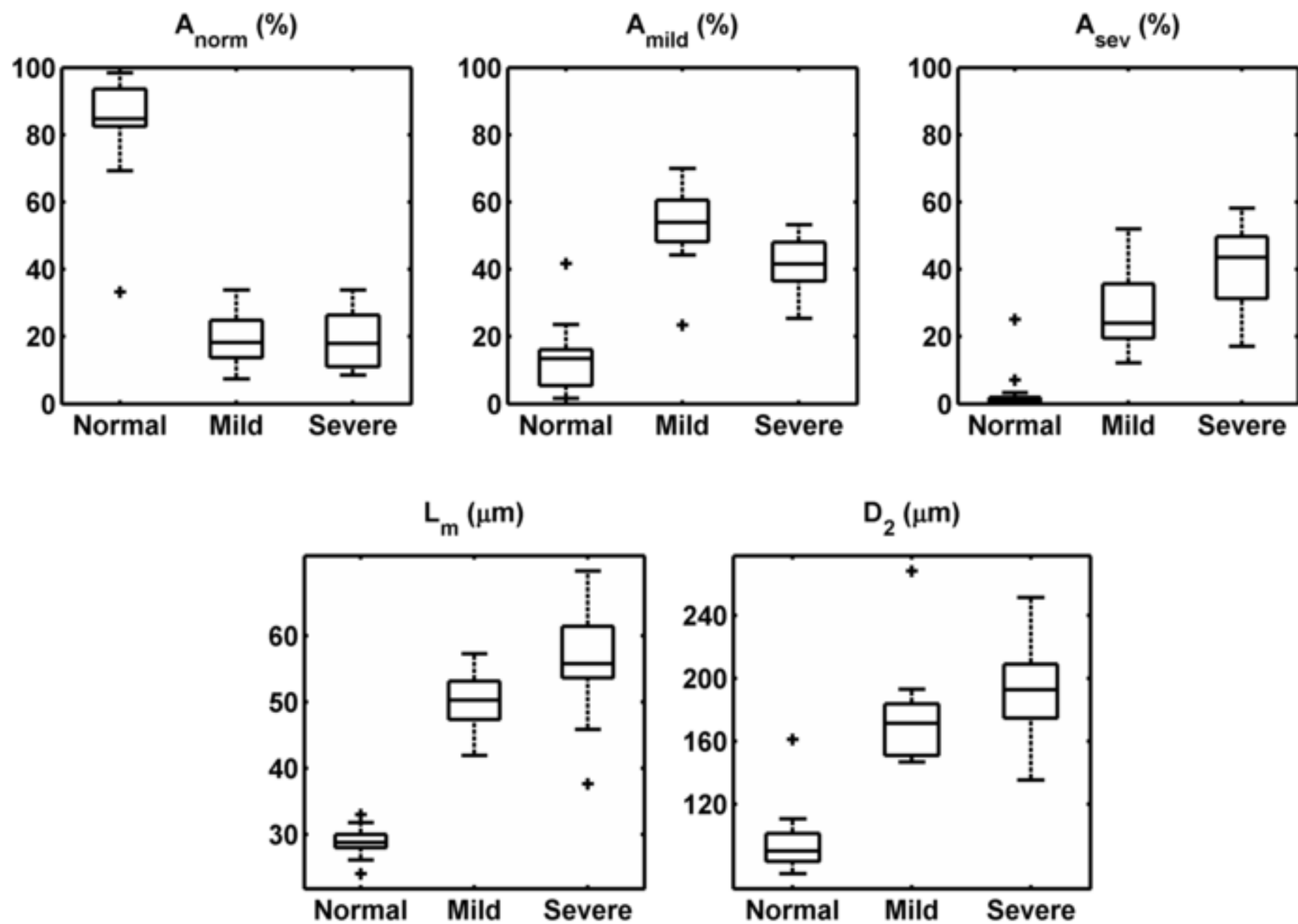


Figure 7

[Click here to download high resolution image](#)

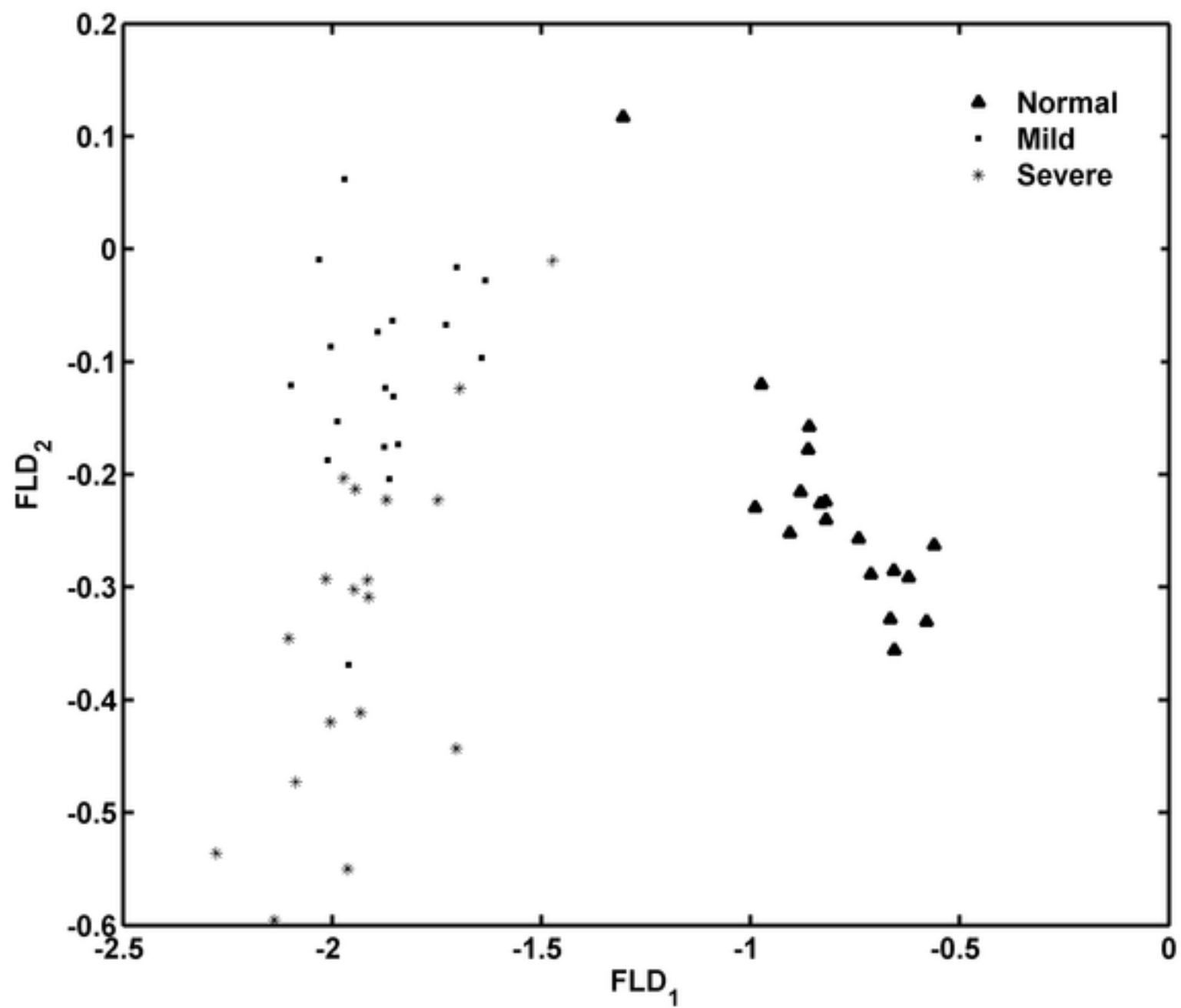


Figure 8
[Click here to download high resolution image](#)

